Chapter 3
Phase Modulated Mode-Locked Figure Eight Fiber Laser

As mentioned in Chapter 2, we purpose design another active mode-locked fiber laser using phase modulator to lock higher frequency pulse train. This Chapter is organized as follows: Section 3-1 introduces the mode-locked figure eight fiber laser(MLF8L). The structure of MLF8L is described in Section 3-2. We derive the theoretical model using ABCD matrix in Section 3-3. In Section 3-4, we present the experimental results. We also give the summary and discussions of our designed MLF8L in Section 3-5.

3-1 Introduction

The phenomenon of mode locking of a laser by an internal phase or amplitude perturba,tion to obtain short optical pulses is well known and has been investigated theoretically and experimentally by several authors. Theoretical studies of the mode-locked laser with an inhomogeneously Doppler-broadened atomic line have been done by DiDomenico [93], Yariv [94], and Crowell [95], all of whom discuss a linearized solution to the problem.More detailed nonlinear calculations for the FM-type mode locking [96] and AM-type mode locking [97] have been presented by

Harris and NIcDuff. In all the above analyses the coupled-mode-equation approachas been used, assuming that the axial modes saturate independently. This has led to a good understanding of mode-locked gas lasers, in particular the He-Ne laser and argon laser [98].Mode locking has also been observed in solid-state Nd:YAG lasers by DiDomenico et *al.* , using an ampli-tude modulator; and in solid-state ruby lasers using an internal amplitude modulator by Deutsch, Pantell, and Kohn [99]. In analyzing these lasers and any other homogeneously broadened lasers, the use of the coupled- mode equations is complicated by the fact that the axial modes do not saturate independently due to the homo-geneous broadening, and also by the fact that a very large number of coupled axial modes are usually generated. Haken and Pauthier have suggested one new analyti- cal approach that can be used for the homogeneous AM-type mode locking.

Therefore , rationally mode-lock ring lasers generate optical pulses at a repetition rate that is *k* time greater than the modulator frequency. Rational mode-locking of erbium-doped fiber lasers at repetition rates of up to 200 GHz have been reported [100].

The Table 3-1 is the some mode-locked fiber laser, the main comparison with their pulsewidth, repetition rate, and their characteristics.

Many kinds of all-optical switching elements such as a nonlinear amplified loop mirror (NALM)[86,87], a nonlinear optical loop mirror (NOLM)[86-87], and a nonlinear polarization rotator have been investigated extensively lately. These devices are useful for generation of ultrashort optical pulses, all-optical demultiplexing, pedestal suppression of

pulses, and so on.

Both of optical time division multiplexing(OTDM) and wavelength division multiplexing(WDM) could be used for extending the capacity of communication system. When the density of the used wavelengths between two near channels is higher and higher in the future, the crosstalk between two wavelength channels will become more serious. Oppositely, OTDM can fully being used in high speed multiplexing. The mode-locked laser is a good technique which can generate short pulse and high power intensity for high speed systems. Laser mode-locking can be classified as active and passive types. Active mode-locked laser is easier to achieve high repetition rate rather than passive mode-locked laser. Active mode-locked laser is able to be adjusted by triggering certain signal to generate harmonic and rational mode-locked laser light output. The repetition rate of pulse trains generated by passive mode-locked laser are mainly controlled with the intracavity properties of component. Among a lot of fiber mode-locked laser structure, figure eight laser(F8L) is one of the famous active mode-locked laser[101].

The structure of mode-locked figure eight fiber laser(MLF8L) was first demonstrated by Duling III[102] to provide clear linear and nonlinear area of light traveling in cavity. Some important controlling factors of mode-locked F8L, for example coupling coefficient of central coupler, has been researched by some groups[103]. Such technique can be applied on measurement system[104] to ensure the high sampling rate. Besides, because the requirements of speed and capacity of communication go high, many researches also have reported related fiber laser for applying in high speed photonic systems[105].

3-2 System Description

In this Section, we design a MLF8L system as shown in Fig. 3-1. With tuning the modulation frequency, we find the fundamental mode locking is 2.5 MHz. Following formula of the free spectral range(FSR): $FSR = \frac{c}{nL}$, where the *n* is 1.46, the *c* is velocity of light and *L* is the cavity length, we find the cavity length about 82.19 m.

The components include EDFA(Lightwave Link, 19”Rack mount, model no. EDFA-1700H), a polarization controllers(PC), an isolator, a phase modulator(Crystal Technology, model no. PM313P) and two couplers. The right side of this system is a nonlinear amplified loop mirror(NALM) which can effectively compress the pulse amplified the power[87]. We use EDFAs to be the gain medium in cavity to get higher power of output port and can enhance nonlinear Kerr effect as the nonlinear refraction index as

$$n = n_0 - n_2 I(t) \tag{3-1}$$

where n_0 is the linear refractive index, n_2 is nonlinear coefficient and *I(t)* is the light intensity. The two EDFAs have gains of 20 dB and 20.1 dB, respectively. The effect on using unbalanced coupler has been demonstrated[47]. The advantage of using unbalanced central coupler is reducing the power loss in ring cavity.

In the left side, we set an isolator to reduce the light coming from the 10% counterclockwise light wave to prevent interfere. The EDFAs in the right side loop of the F8L also have isolators inside to suppress the counterclockwise light propagation. Besides, we use a phase modulator to generate the active mode locking. The phase mode-locked laser for change of phase is very sensitivity. We directly to control and tuning the phase change by phase modulator. The phase modulator can easily generate high quality of harmonic and rational mode-locked laser. Besides, there are polarization-maintain fibers linked in phase modulator. The PC is used to tune the polarization state in this system. With properly control the condition of polarization in F8L cavity, we can have a better output pulses. In this paper, we only give radio frequency(RF) signal to modulate the phase modulator. When we adjust the output level and frequency of phase modulator, the pulsewidth of the laser can be varied. A 3 dB 2x2 coupler at last is connected to a high speed sampling oscilloscope to see the pulse time response. The another port of 3 dB coupler use matching index oil to avoid the light reflection because of different index between core and air.

3-3 Theoretical Model

The internal phase modulator introduces a sinusoidally varying phase perturbation $\delta(t)$ such that the round-trip transmission through the modulator is given by[106]

$$\exp[-j\delta(t)] = \exp(-j2\delta_c)\cos\omega_m t \tag{3-2}$$

where ω_m is the modulation frequency and the effective single-pass phase retardation of the modulator δ_c

$$\delta_c = \left(\frac{L}{a}\frac{2}{\pi}\sin\frac{a}{L}\frac{2}{\pi}\right)\left(\cos\frac{Z_0\pi}{L}\right)\delta_m \tag{3-3}$$

where L is the length of the cavity, a the length of the modulator crystal, Z_0 is the distance of the modulator to a mirror, and δ_m the peak phase retardation through the crystal.

We can also consider the more general case, when the pulse goes through the modulator at a phase angle θ from the ideal case. The transmission through the modulator can now be written as

$$\begin{aligned}\exp[-j\delta(t)] = \exp(&\mp j2\delta_c\cos\theta \pm j2\delta_c\sin\theta(\omega_m t) \\ &\pm j\delta_c\cos(\omega_m{}^2 t^2))\end{aligned} \tag{3-4}$$

3-3-1 FM signal fed PM

We can now get the expressions for the pulsewidth[106]

$$\tau_p(FM) = \frac{\sqrt{2\sqrt{2}\ln 2}}{\pi}\left(\frac{g_0}{\delta_c}\right)^{1/4}\left(\frac{1}{f_m \Delta f}\right)^{1/2} \tag{3-5}$$

where

$$g_0 = \frac{1}{2}\ln\frac{1}{R} - \frac{1}{4}\ln\left[1 - \frac{16\ln 2\,\delta_c {f_m}^2}{\Delta f_p^2} + \frac{1}{2}\left(\frac{16\ln 2\,\delta_c {f_m}^2}{\Delta f_p^2}\right)^2\right] \tag{3-6}$$

where R is the effective (power) reflection of a mirror and includes all losses and bandwidth Δf_p (FM)

$$\Delta f_p(FM) = \frac{\sqrt{2\sqrt{2}\ln 2}}{\pi}\left(\frac{\delta_c}{g_0}\right)^{1/4}\left(f_m \Delta f\right)^{1/2} \tag{3-7}$$

3-3-2 AM signal fed PM

We can now get the expressions for the pulsewidth[106]

$$\tau_p(AM) = \frac{\sqrt{\sqrt{2}\ln 2}}{\pi}\left(\frac{g_0}{\delta_c}\right)^{1/4}\left(\frac{1}{f_m \Delta f}\right)^{1/2} \tag{3-8}$$

where

$$g_0 = \frac{1}{2}\ln\frac{1}{R} - \frac{1}{2}\ln\left[1 - 16\ln 2\,\delta_c\left(\frac{f_m}{\Delta f_p}\right)^2\right] \qquad (3\text{-}9)$$

where bandwidth Δf_p (AM)

$$\Delta f_p(AM) = \frac{\sqrt{\sqrt{2}\ln 2}}{\pi}\left(\frac{\delta_c}{g_0}\right)^{1/4}(f_m \Delta f)^{1/2} \qquad (3\text{-}10)$$

A simple interpretation can be given of the mode- locking process. We saw previously that the passage of the pulse through the active medium narrowed the spectral width of the pulse or alternatively changed the width of the pulse. One can now visualize this pulse going through an amplitude modulator where the pulse is shortened due to the time-varying transmission of the modulator. The equilibrium condition between the lengthening due to the active medium and shortening due to the modulator determines what the steady-state pulsewidth will be. A similar interpretation can be given for FM modulation, but it is now easier to visualize the process in the frequency domain. When the pulse passes through the Phase modulator, a frequency chirp is put on the pulse. This frequency chirp increases the spectral width of the pulse and an equilibrium state is reached where the increase in spectral width due to the modulator is equal to the narrowing of the spectral width due to the active medium. It is interest- ing to notice that this equilibrium condition requires a steady-state

frequency chirp on the pulse and further that the pulse envelope and frequency chirp contribute equally to the spectral width of the pulse (Le., *a!* = 0). The interpretation that is usually given for mode locking in an inhomogeneously broadened laser is that the modulator introduces some coupling between adjacent axial modes and that this coupling locks the phases of these modes in such a way as to give short pulses (and hence the terms mode locking or phase locking). This interpretation is not useful for the homogeneously broadened laser, since most of the axial modes are not present in the free-running laser. There are usually only a few axial modes, mostly due to spatial inhomogeneity and hence the term mode locking is somewhat of a misnomer, but we will retain it with a somewhat broadened meaning.

3-4 Analysis of Results

We used the structure of MLF8L not only get the nice output, but also analyze the results of detuning the modulation frequency. We have tried to adjust the modulation frequency and amplitude level to observe the change of pulse trains. Fig. 3-3 depicts the theoretical and experimental results. From observing the theory curve(solid line), we find the range of pulsewidth of 37 ps to 18.2 ps following modulation frequency to display two order decay. This is easily to understand by Eq. (3-17), although we

can’t solute the analytic solution. Of course, if we use different parameters in other elements, the curvature may be shifted or change, but the trends of two order decay following the modulation frequency to become large. In Fig. 3-3, we have proved the theoretical and experimental curves are very close. We also can depict the theoretical chirp parameter of our designed MLF8L in Fig. 3-4. At modulation frequency is 1.0249777 GHz, the pulsewidth is 40 ps and the chirp parameter is about 3.1×10^{-3}. The chirp parameters vary with modulation frequency from 1 GHz to 2.7 GHz are within 2.14×10^{-3}.

In next subsection, we use the modulation frequency(MF) of 2.4787836 GHz and amplitude level(AL) of 16.4 dBm to generate 10 Gb/s pulse train.

3-4-1 10 GHz Pulse Train Generation

We use Agilent 86100A high speed sampling oscilloscope to measure the time response of MLF8L. When tuning the frequency of 4 times fundamental MF, the fourth order harmonic mode-locked laser is generated as shown in Fig. 3-5. This lasing spectrum is shown in Fig. 3-6. The bandwidth of lasing spectrum is 6 nm.

The variation of the repetition rate by detuning MF is shown in Fig. 3-7. The largest value 10.2 GHz of repetition rate at MF of 2.4787836 GHz and amplitude level of 16.4 dBm. Besides, we find the maximum change range is 0.24 GHz at AL of 16.4 dBm.

Fig. 3-8 depicted the curve of MF versus pulsewidth. In our

experimental results, the pulsewidths become broaden when far away MF of 2.478783624 GHz.

The rise time and falling time are the important parameters of pulse shapes. The rise time, falling time and pulsewidth can directly affect the bit error rate because of intersymbol interference. Thus, we have to understand the change of pulse. The rise time and falling time vary with MF as shown in Fig 2-9 and Fig 2-10, respectively. The rise time become flat when MF are far away 2.478783570 GHz. Oppositely, the falling time can be sharper. The root-mean-spuare(RMS) jitter become worse except 2.47878363 GHz as shown in Fig. 2-11. At The worst RMS jitter is 20.5 ps, and the optimal RMS jitter can achieve 16.32 ps. We easily find the minimum jitter occurs at the shortest pulsewidth.

3-4-2 20 GHz Pulse Train Generation

Fig.3-12 is the pulse train of 20 GHz when MF of 2.49171142 GHz. Because of the rational mode-locking, the pulse train is not equalization. The lasing spectrum is shown in Fig. 3-13 and the spectrum spread about 6 nm.

We can record the repetition rate vary with detuning MF in Fig. 3-14. The maximum change range of detuning AL of 16.4 dBm are 1.3 GHz. We can also find the pulsewidth change in Fig. 3-15. The shortest pulsewidth of 20.26 ps is at MF of 2.491710466 GHz and AL of 18 dBm. The trend of the change of the rise time in Fig. 3-16 and Fig. 3-17. The shortest rise time is about 16.4 ps at MF of 2.491710442 GHz and AL of 16.4 dBm. Following

to tuning lower AL and far away 2.491710341 GHz, the rise time become more flat. In Fig. 3-17, the trend of falling time is just opposite to rise time. In Fig. 3-18, the RMS jitter has the unregulated variation, but we can find the minimum value of 11.77 ps.

3-4-3 40 GHz Pulse Train Generation

In near the 2.5711934 GHz, we can achieve the 40 GHz pulse train. The waveform and optical spectrum are shown in Fig. 3-19 and Fig. 3-20, respectively. The lasing spectrum is spread over 7 nm. We can use 16.4 dBm to generate repetition rate of 40 GHz by detuning the frequency of 2.5711934 GHz. In Fig. 3-21, the variation range of repetition rate of 16.4 dBm are 1.2 GHz. The pulsewidth vary with modulation frequency is shown in Fig. 3-22. We know the shortest pulsewidth is 18.3 ps with AL of 16.4 dBm and MF of 12.000205 GHz. The rise time and falling time depict in Fig. 3-23 and Fig. 2-24. The shortest rise time is about 11.27 ps at MF of 2.571193320 GHz and AL of 16.4 dBm. Following to tuning lower AL and far away 2.571193570 GHz, the rise time become more flat. The RMS jitter is shown in Fig. 3-25. The RMS jitter has the optimal value of 8.37 ps.

In next subsection, we trigger the 50 GHz pulse train using MF of 2.6820745 GHz and AL of 16.4 dBm.

3-4-4 50 GHz Pulse Train Generation

When the modulation frequency is 2.6820745 GHz and 16.4 dBm, the 50 GHz pulse train can be generated as shown in Fig. 3-26. Because of limited by sensitivity of oscilloscope, the 50 GHz pulse train is not such clear. The 50 GHz lasing spectrum is shown in Fig. 3-27, we know the lasing spectrum is about 6 nm. In Fig. 3-28, the little variation of repetition rate can be found. We know the maximum value is 50.2 GHz and minimum value is about 49.87 GHz. In Fig. 3-29, we find the narrowest pulsewidth is 16.67 ps. The trend of far away 2.68207548 GHz become more broaden. As shown in Fig. 3-30 and Fig. 3-31, the rise time and falling time have the opposite change. We also get the narrowest values of rise time and falling time are 1.148 ps and 1.3 ps, respectively. The RMS jitter has the optimum value of 5.174 ps at modulation frequency of 2.68207560 GHz as shown in Fig. 3-32.

3-5 Summary

In this Chapter, we have demonstrated a new structure of using phase modulated MLF8L. We have trigger the mode-locked laser of repetition rate of 10 GHz, 20 GHz, 40 GHz and 50 GHz with modulation frequency of 2.4787836 GHz, 2.49171142 GHz, 2.5711934 GHz, and 2.6820745 GHz, respectively. With time-domain ABCD matrix, we budget pulsewidth and chirp parameter of the mode-locked laser cavity. In above experiment, we have known the methods of tuning fitting pulse shape. Besides, we have

got RMS jitter of 5.174 ps at modulation frequency of 2.58207560 GHz. The property of this condition is very beneficial to optical transmission system.

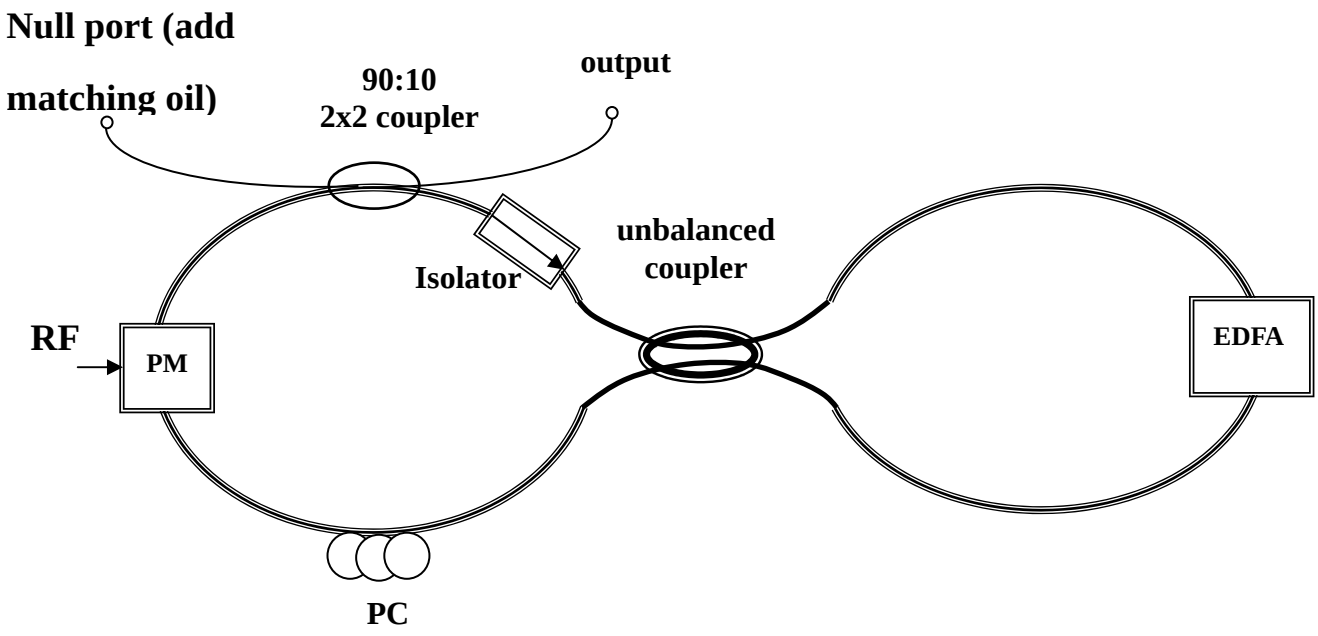

Fig. 3-1 The structure of a phase-modulated MLF8L

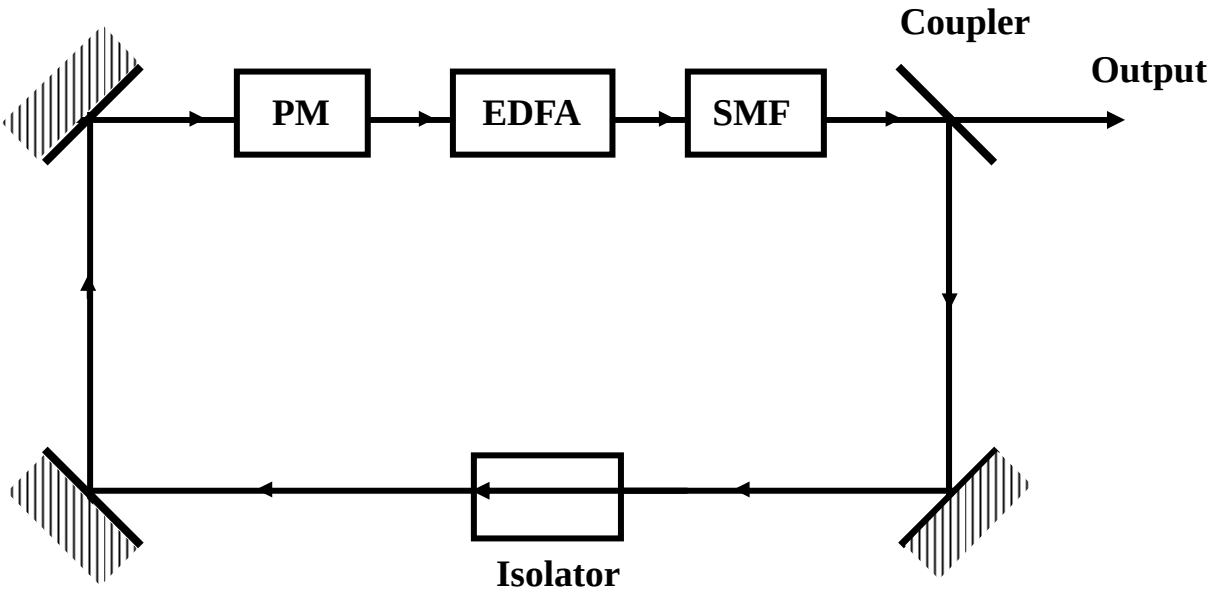

Fig. 3-2 The schematic expressions of the MLF8L using time-domain ABCD matrix

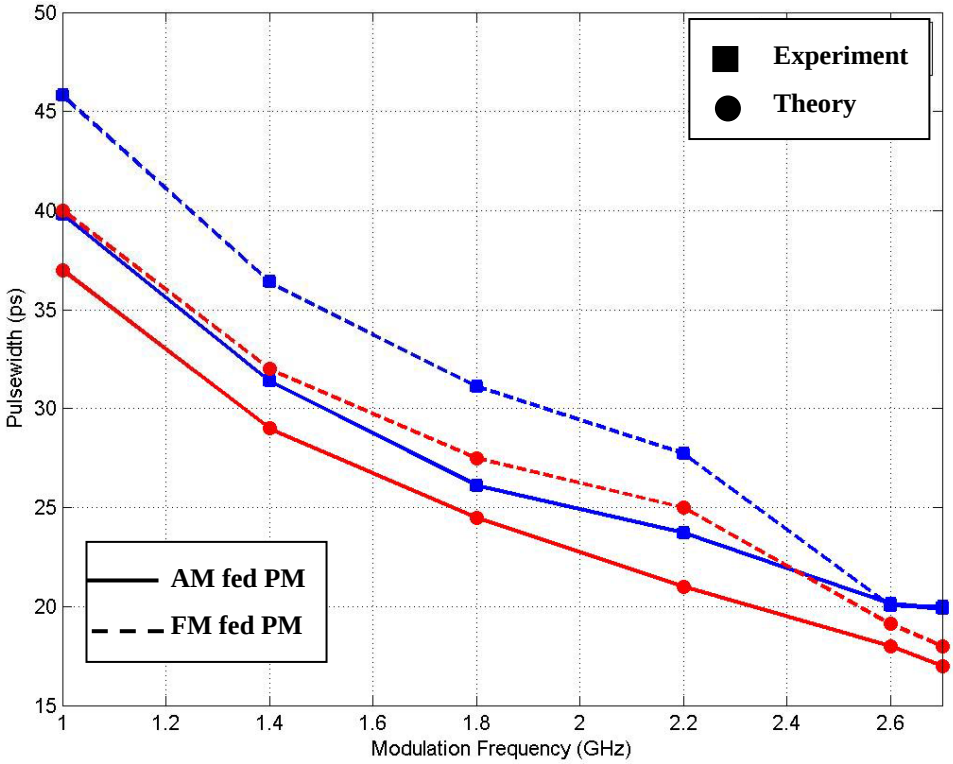

Fig. 3-3 The diagram of comparing with theory and experiment

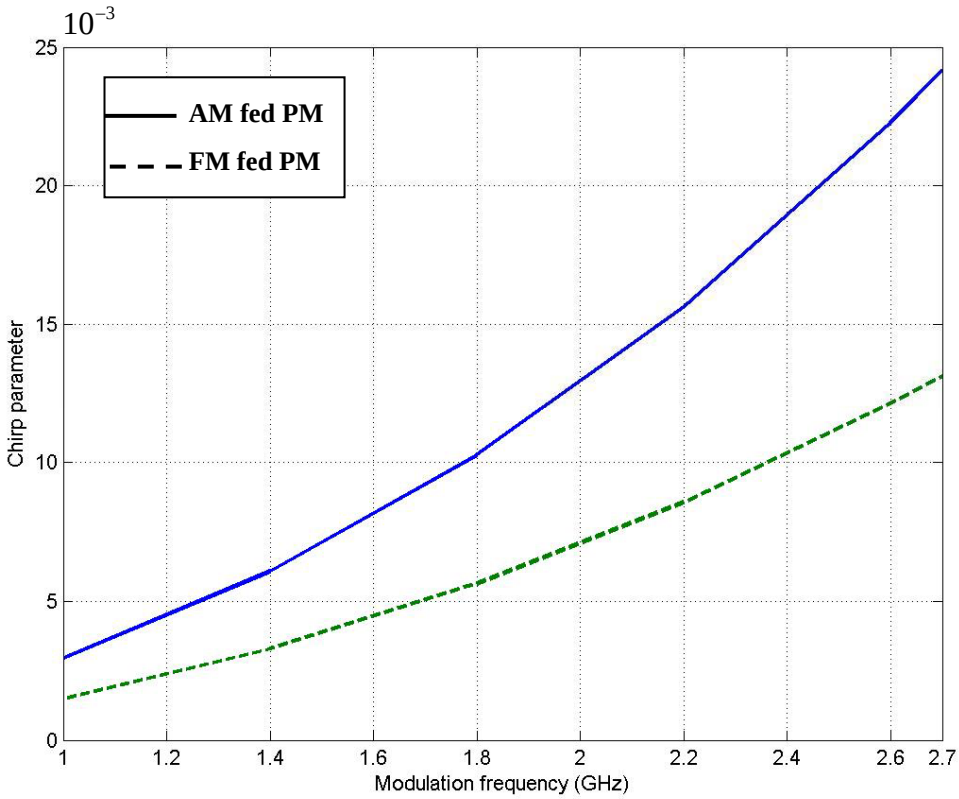

Fig. 3-4 The chirp parameter change with modulation frequency

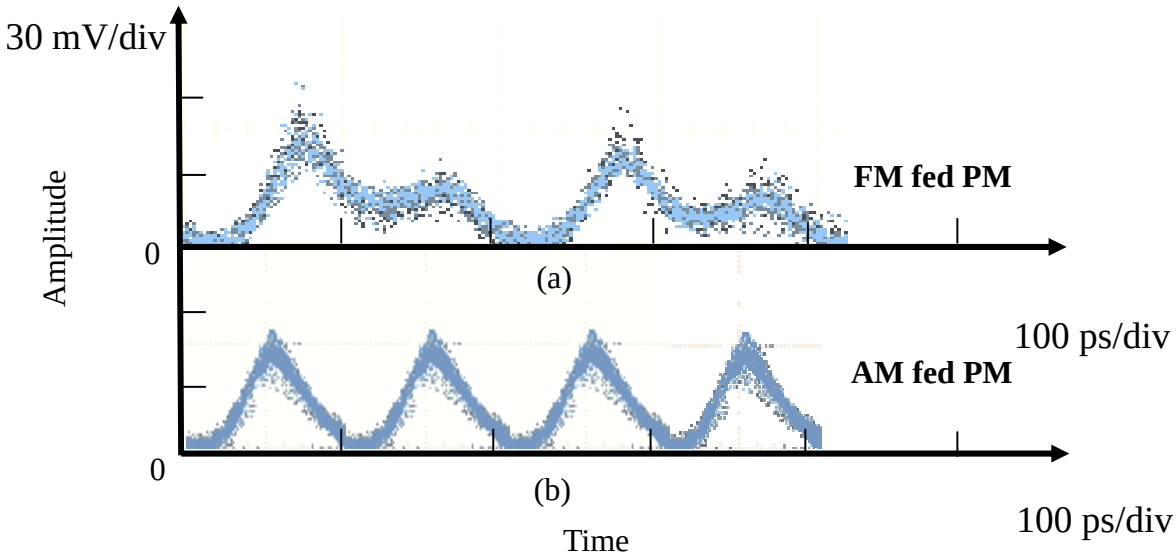

Fig. 3-5 (a)The 10GHz pulse train of MLF8L with modulation frequency of 2.4787836 GHz and amplitude 16.4 dBm

(b) The 10GHz pulse train of MLF8L with modulation frequency of 2.4787836 GHz and ac FM modulation index 0.05

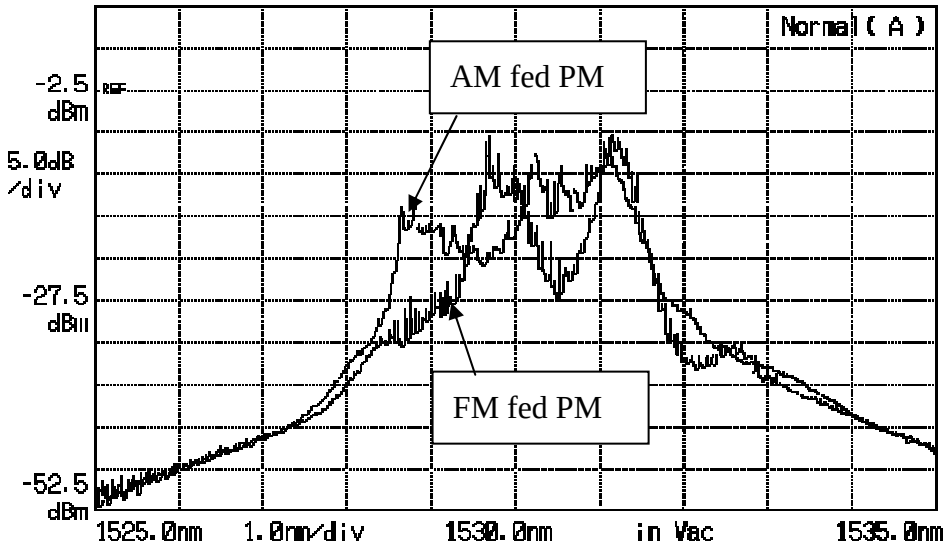

Fig. 3-6 The 10 GHz lasing spectrum with modulation frequency of 2.4787836 GHz

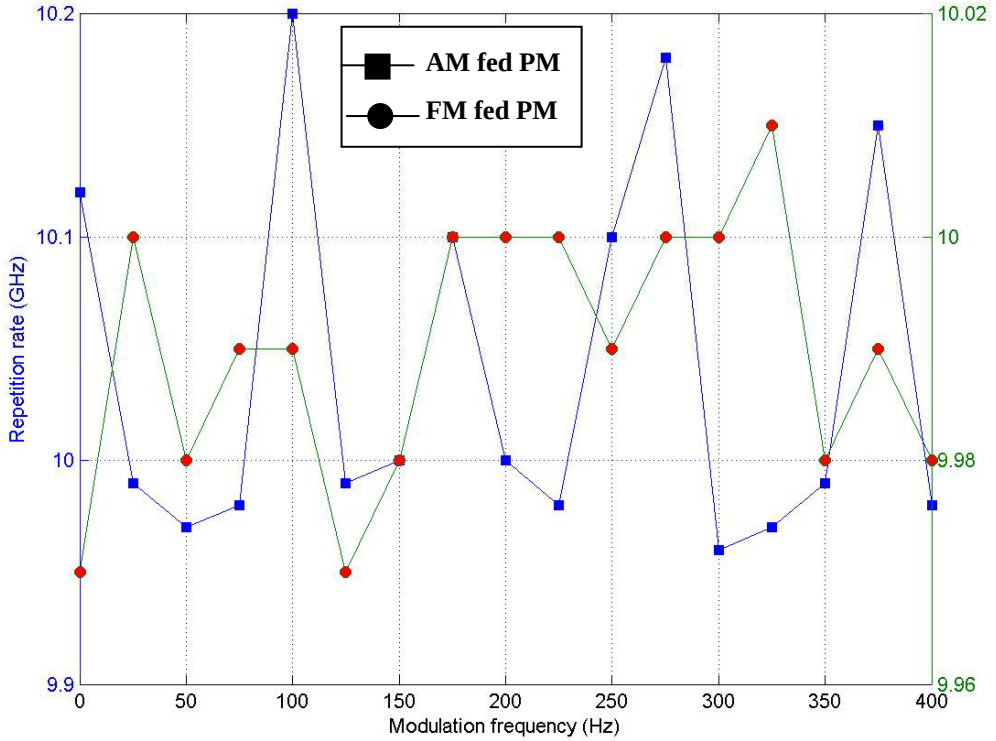

Fig. 3-7 The repetition rate vs. modulation frequency with amplitude level (offset=2.4787834 GHz)

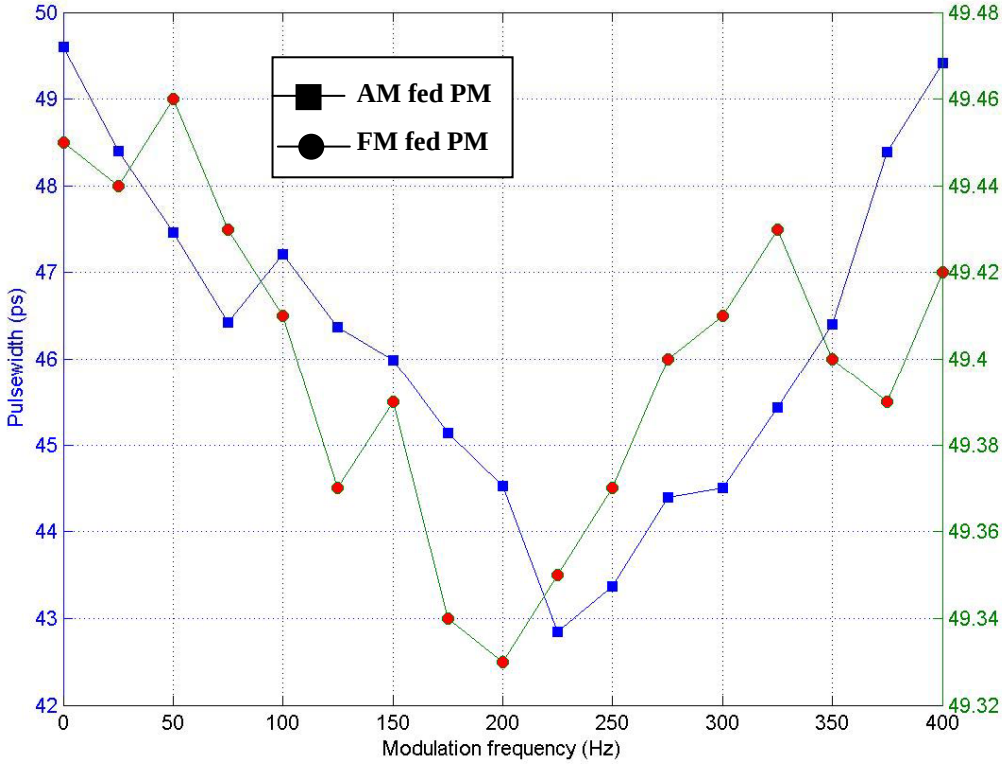

Fig. 3-8 The pulsewidth vs. modulation frequency (offset=2.4787834 GHz)

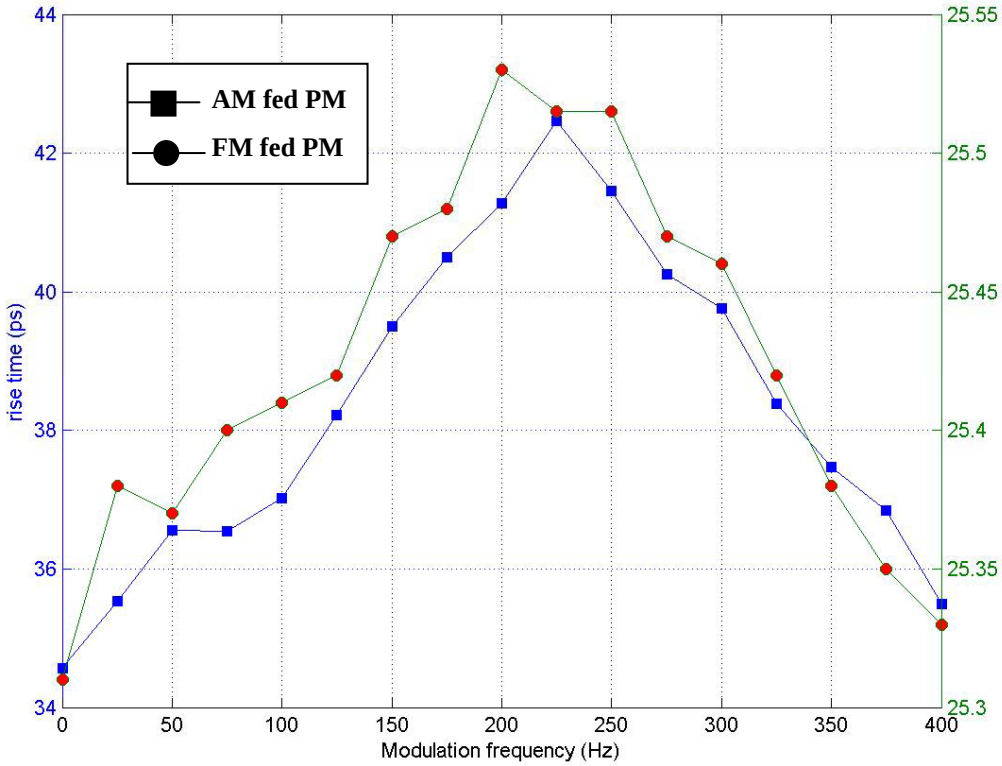

Fig. 3-9 The rise time vs. modulation frequency (offset=2.4787834 GHz)

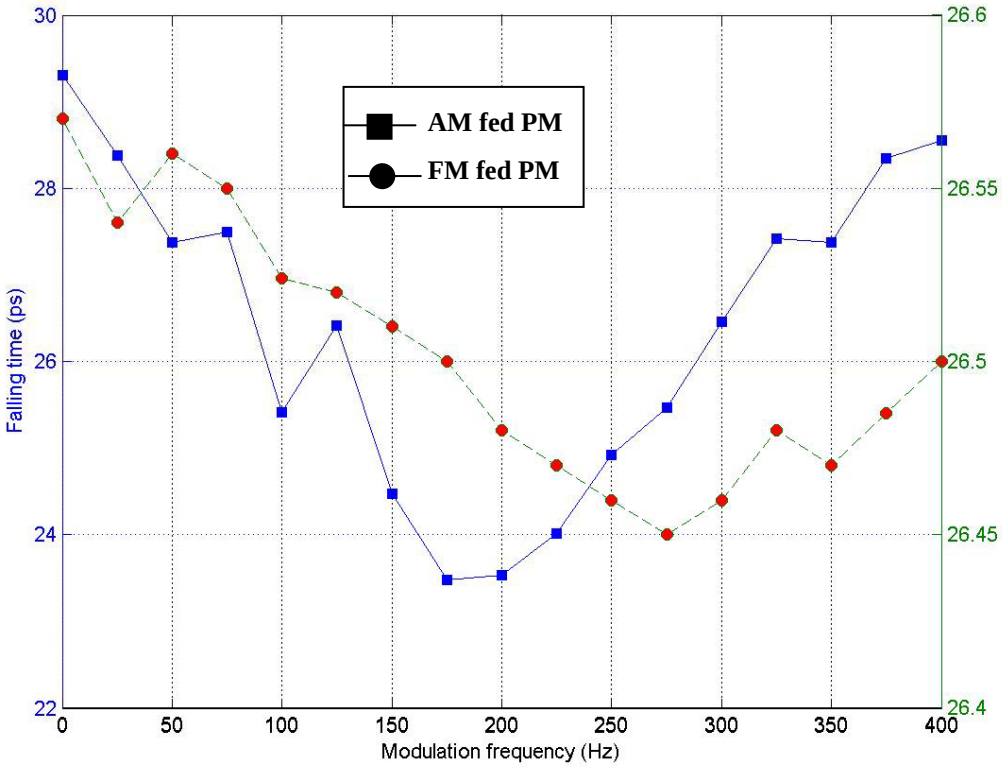

Fig. 3-10 The falling time vs. modulation frequency (offset=2.4787834 GHz)

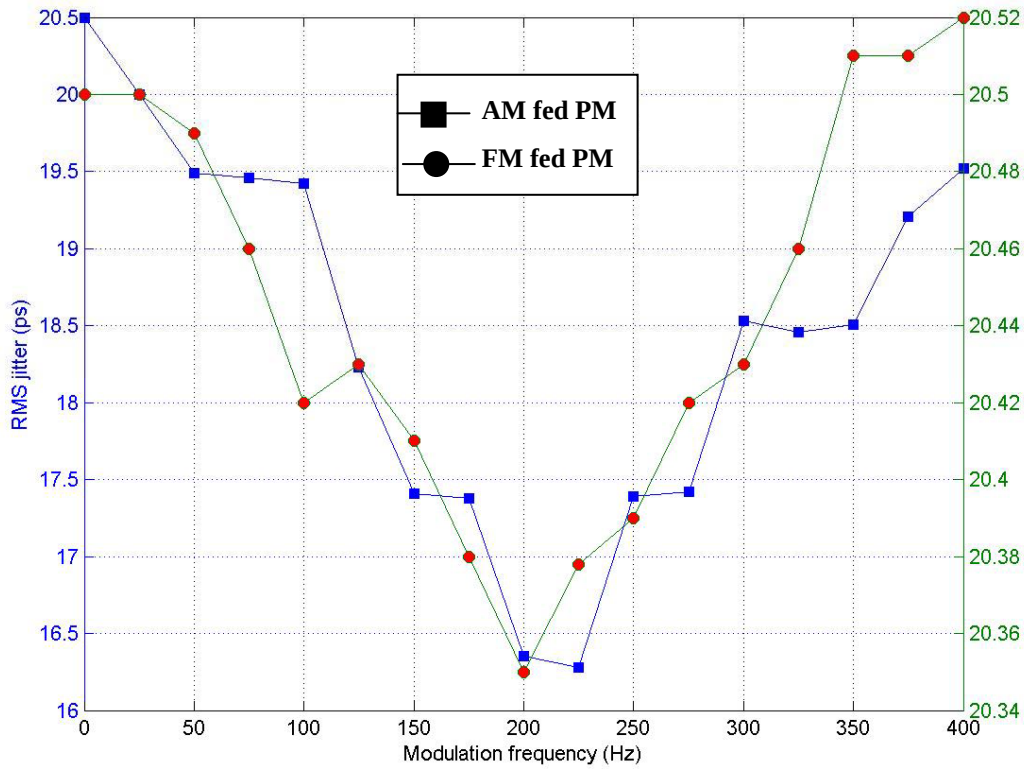

Fig. 3-11 The RMS jitter vs. modulation frequency (offset=2.4787834 GHz)

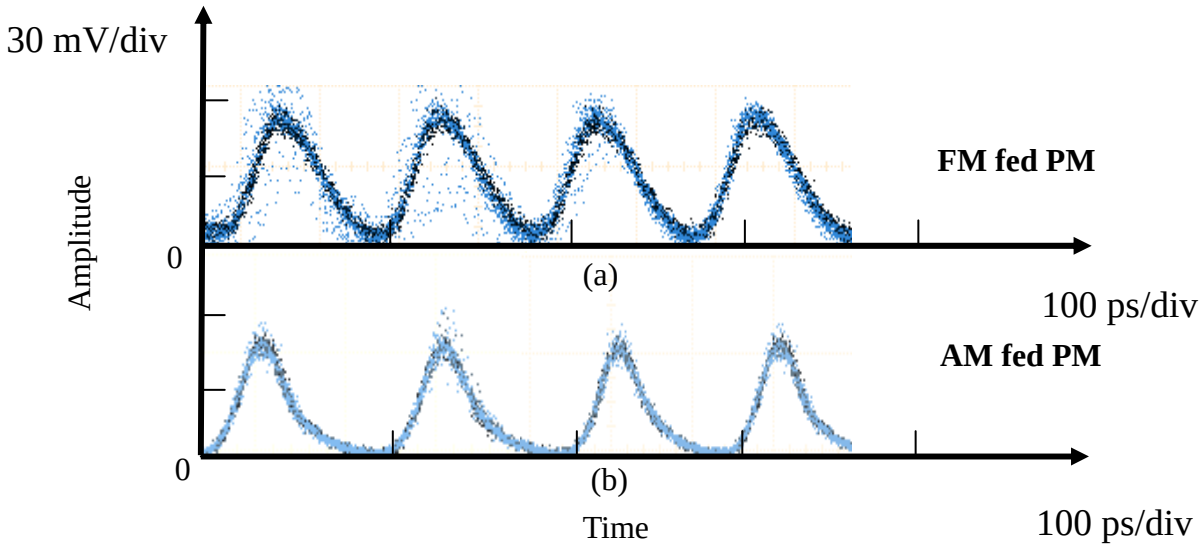

Fig. 3-12 (a)The 20GHz pulse train of MLF8L with modulation frequency of 2.49171142 GHz and amplitude 16.4 dBm

(b) The 20GHz pulse train of MLF8L with modulation frequency of 2.49171142 GHz and ac FM modulation index 0.12

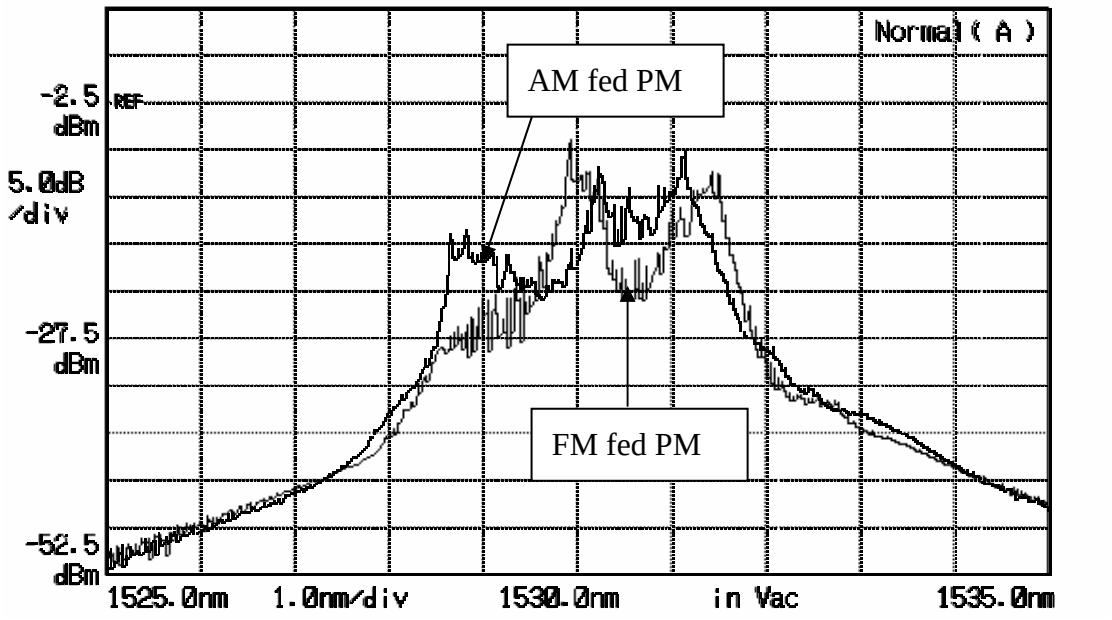

Fig. 3-13 The 20 GHz lasing spectrum with modulation frequency of 2.49171142 GHz

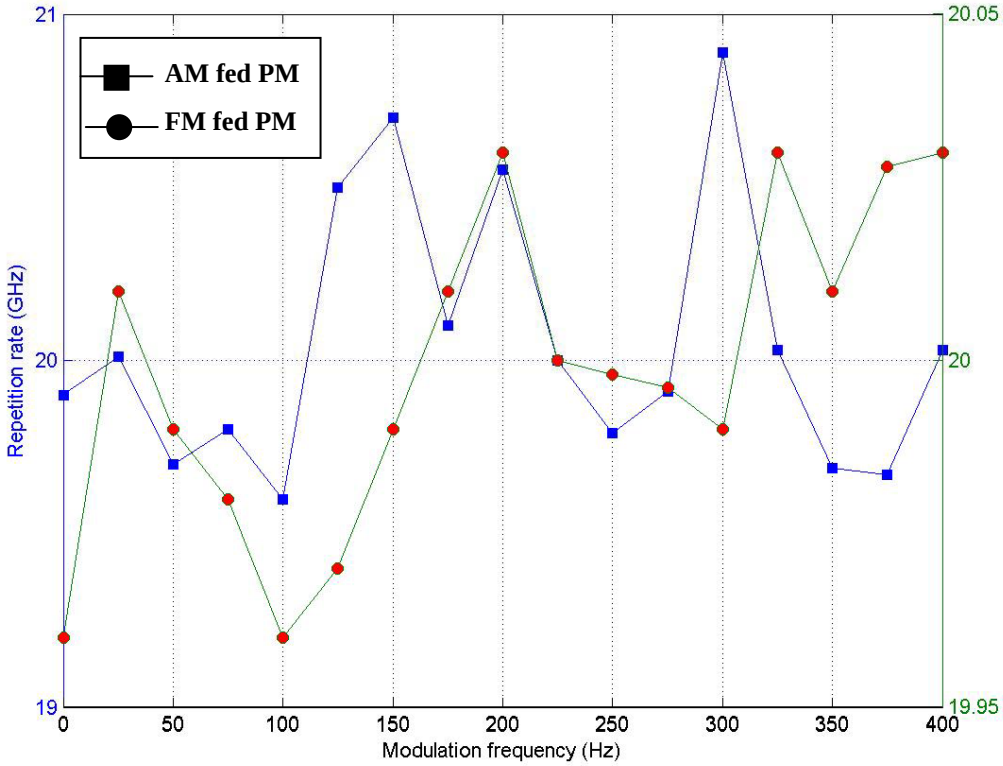

Fig. 3-14 Change of repetition rate by detuning modulation frequency (Offset=2.49171002 GHz)

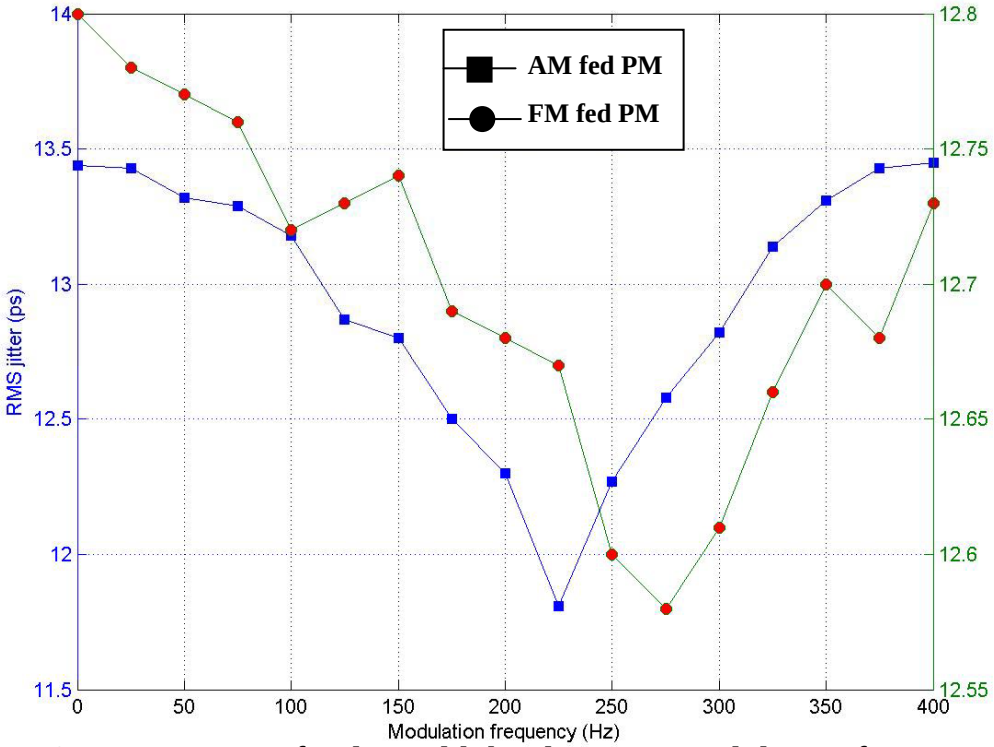

Fig. 3-15 Variation of pulsewidth by detuning modulation frequency (Offset=2.49171002)

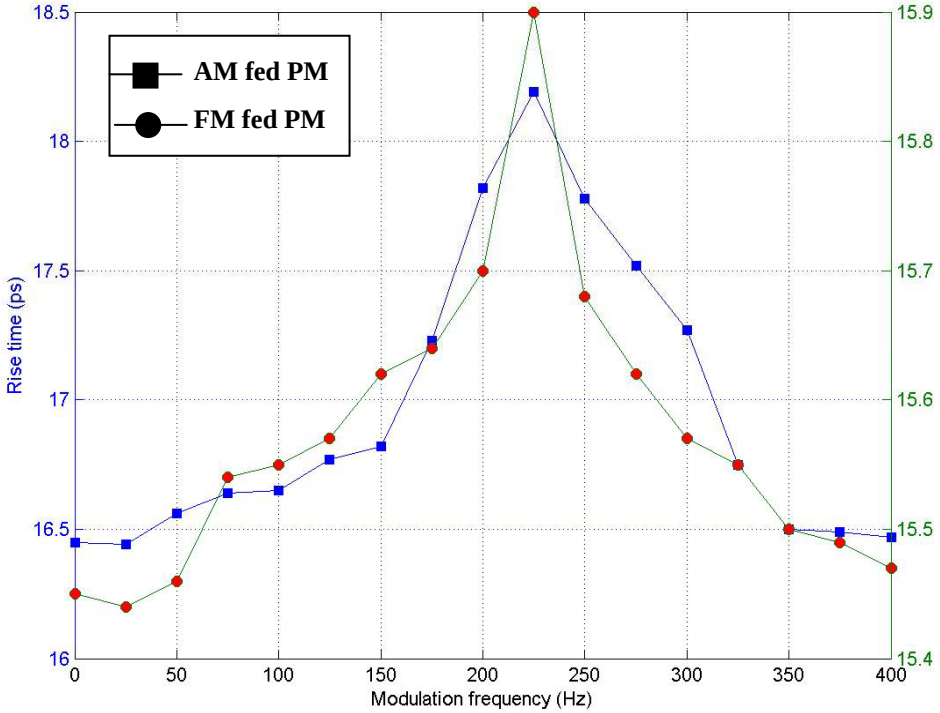

Fig. 3-16 Variation of rise time by detuning modulation frequency (Offset=2.49171002 GHz)

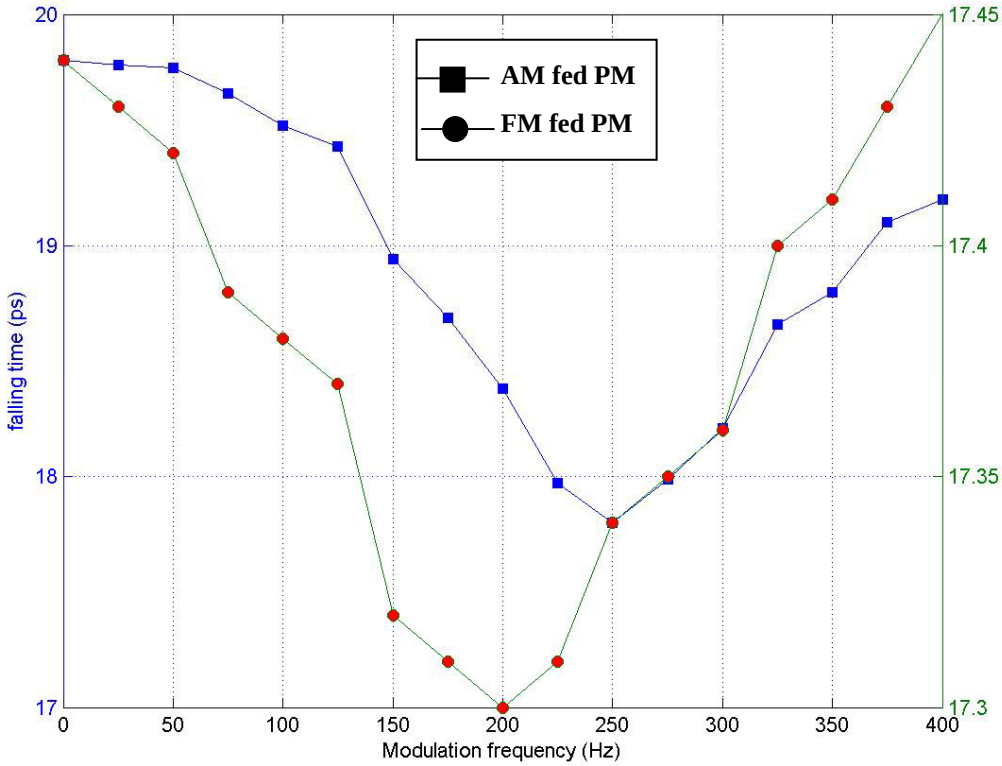

Fig. 3-17 Variation of falling time by detuning modulation frequency.

(Offset=2.49171002 GHz)

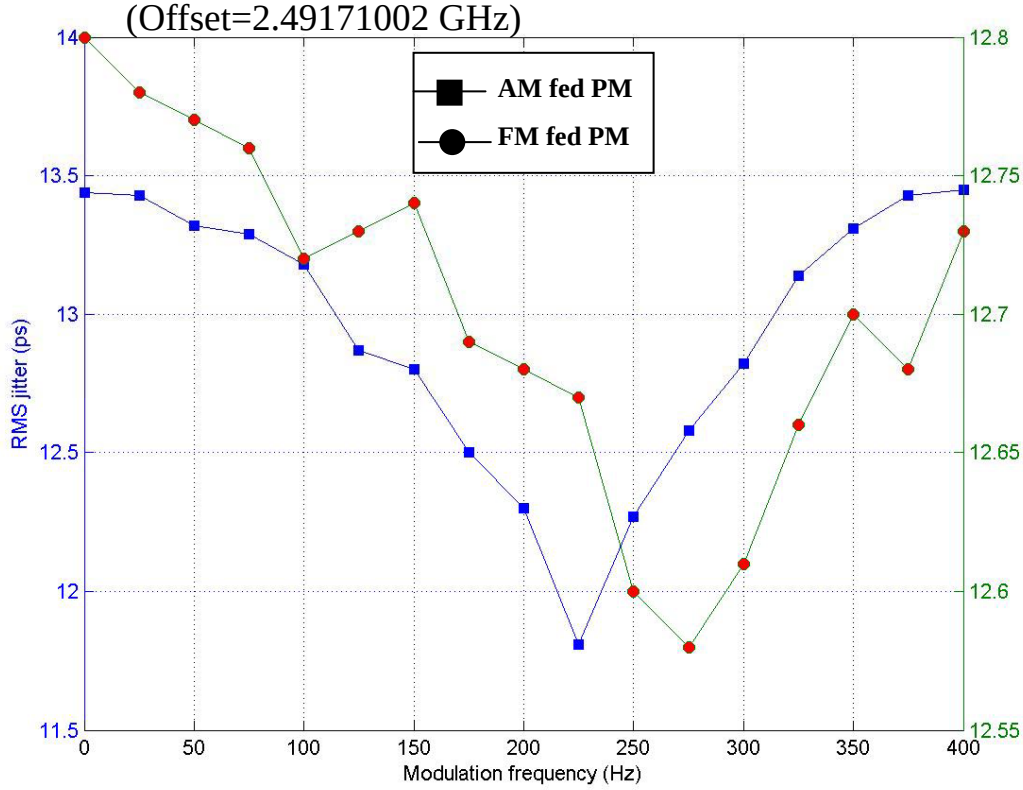

Fig. 3-18 Variation of RMS jitter by detuning modulation frequency

(Offset=2.49171002 GHz)

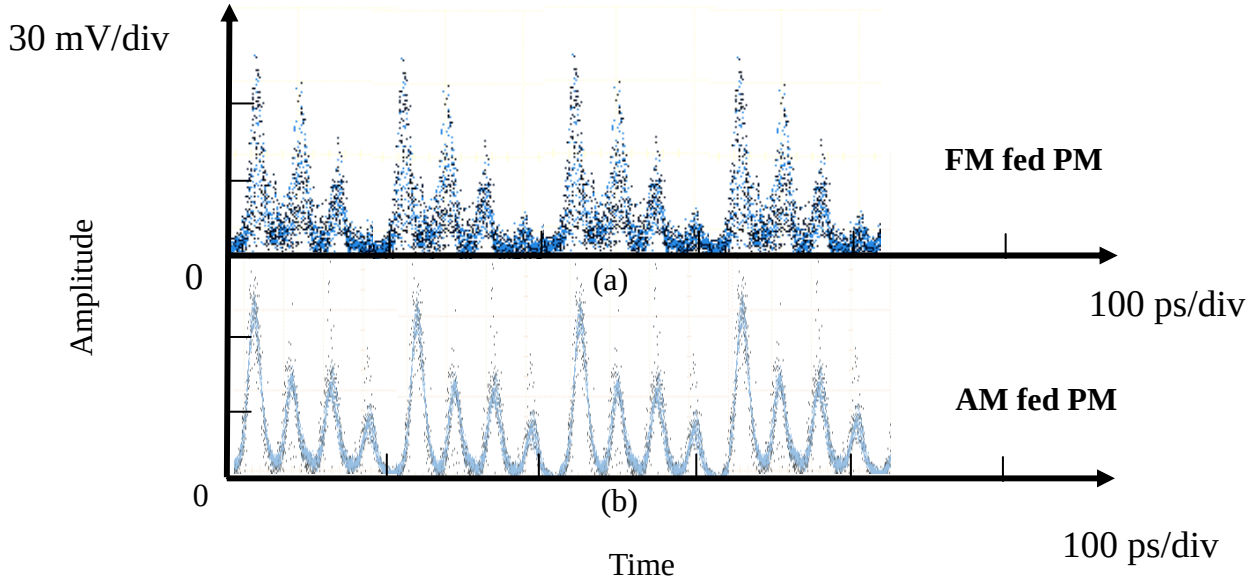

Fig. 3-19 (a)The 40GHz pulse train of MLF8L with modulation frequency of 2.5711934 GHz and amplitude 16.4 dBm

(b) The 40GHz pulse train of MLF8L with modulation frequency of 2.5711934 GHz and ac FM modulation index 0.31

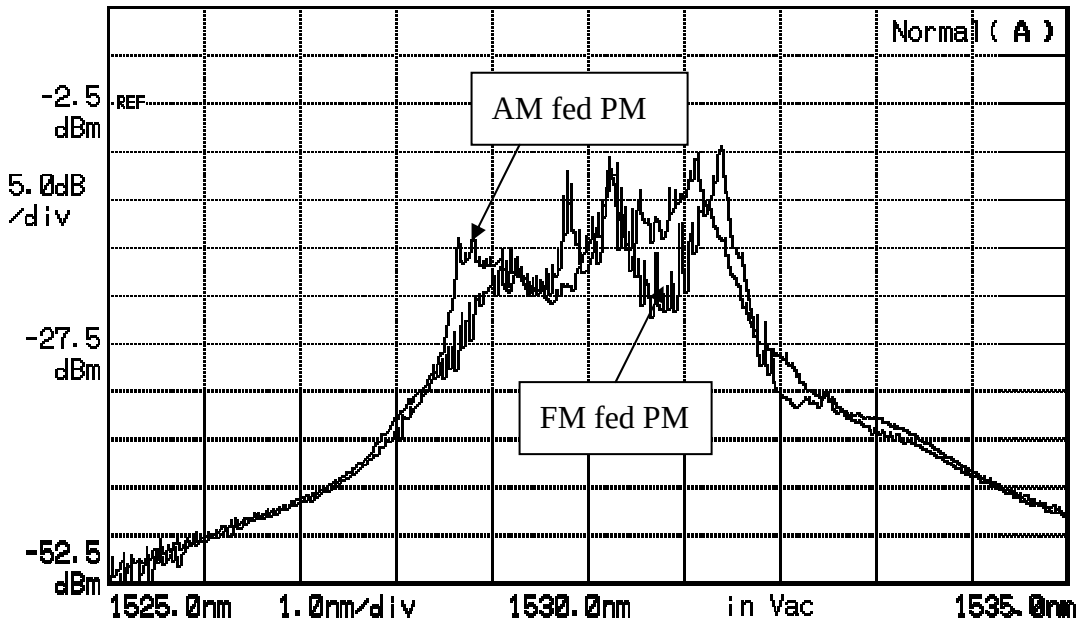

Fig. 3-20 The lasing 40GHz spectrum with modulation frequency of 2.5711934 GHz

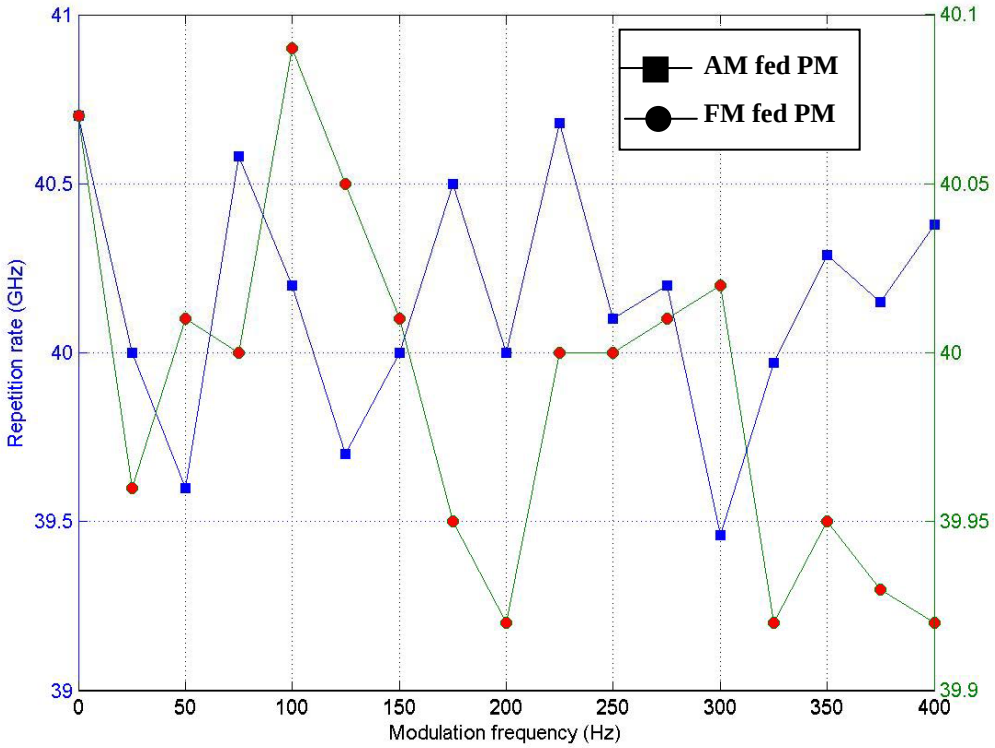

Fig. 3-21 Change of repetition rate by detuning modulation frequency.

(Offset=2.57119327 GHz)

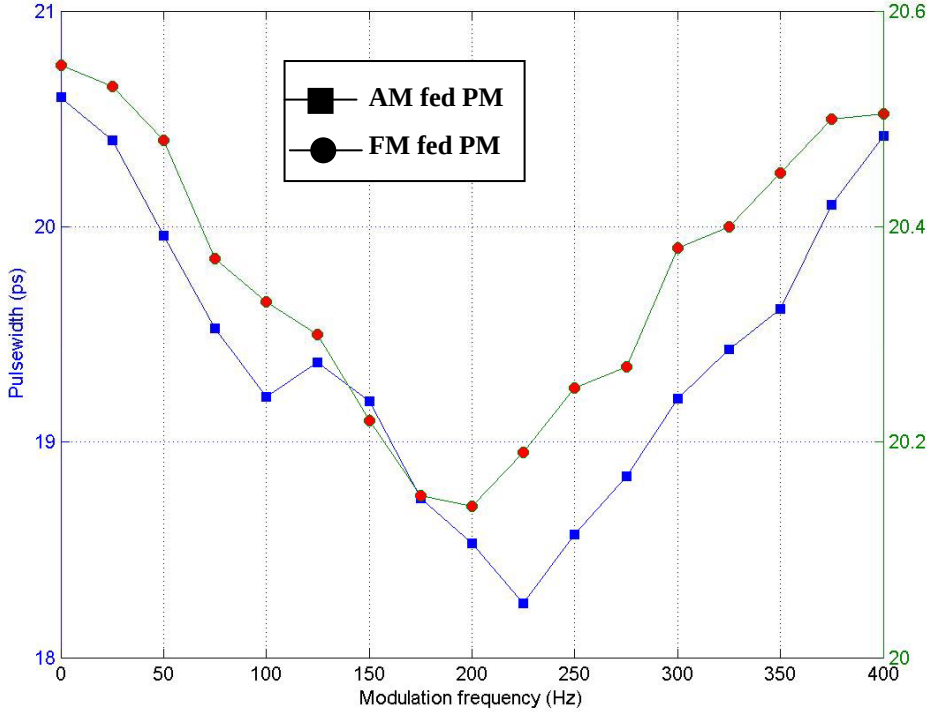

Fig. 3-22 Variation of pulsewidth by detuning modulation frequency

(Offset=2.57119327 GHz)

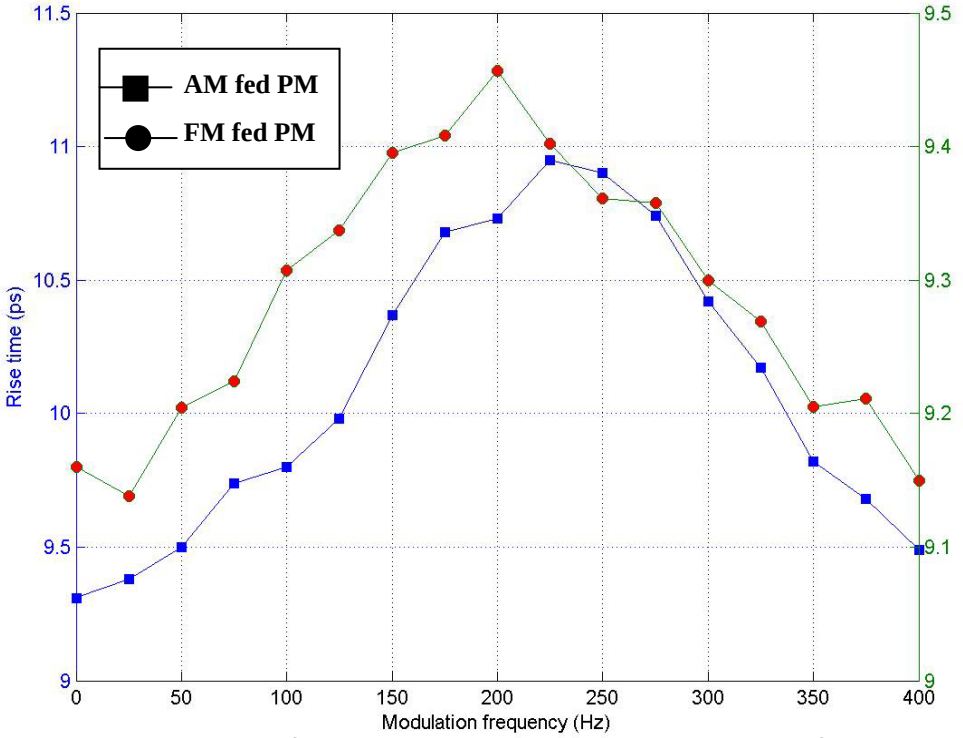

Fig. 3-23 Variation of rise time by detuning modulation frequency.

(Offset=2.57119327 GHz)

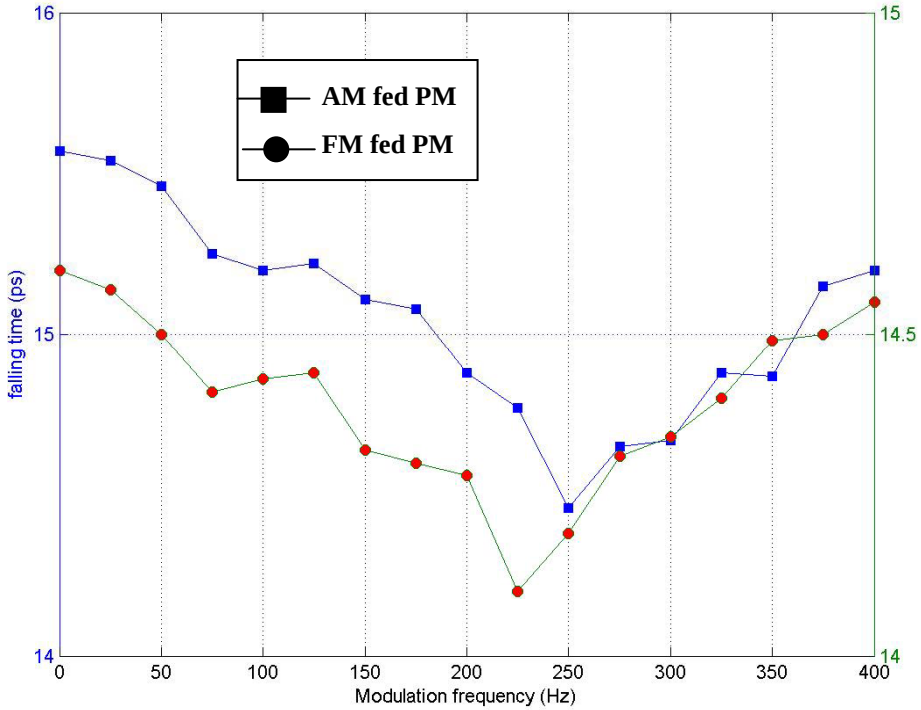

Fig. 3-24 Variation of falling time by detuning modulation frequency

(Offset=2.57119327 GHz)

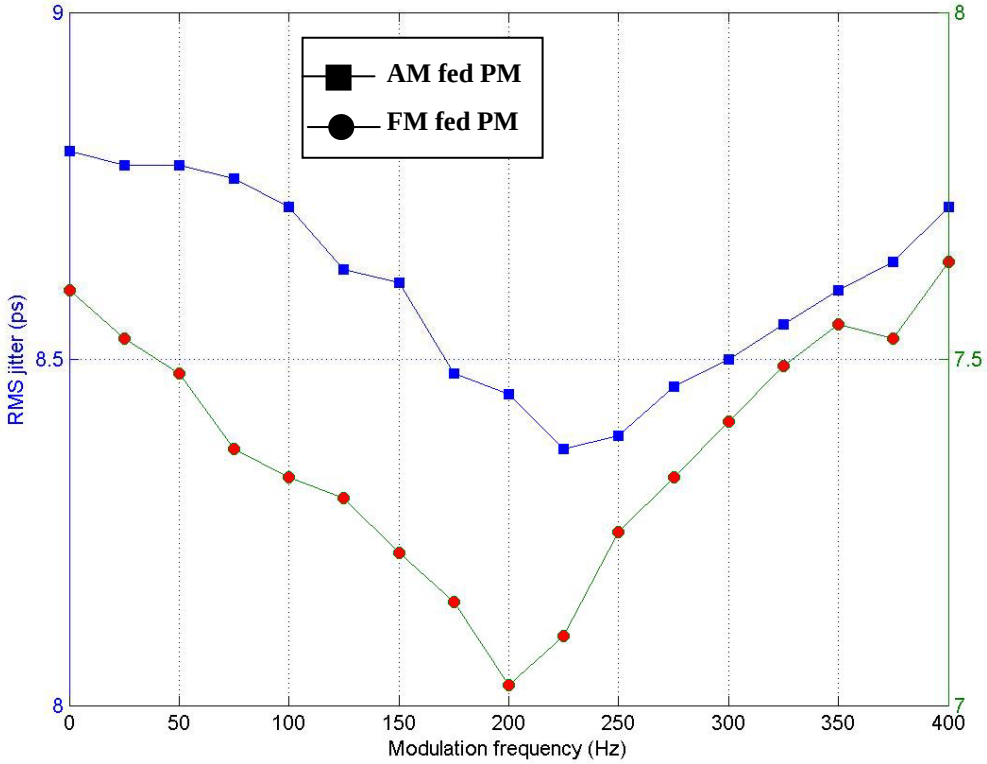

Fig. 3-25 Variation of RMS jitter by detuning modulation frequency (Offset=2.57119327 GHz)

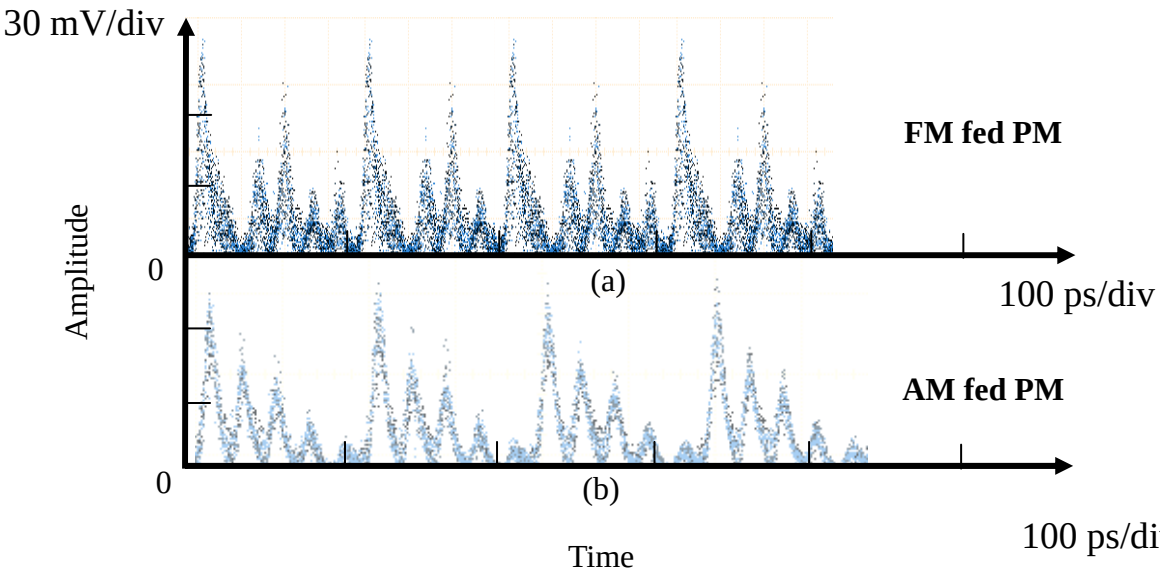

Fig. 3-26 (a)The 50GHz pulse train of MLF8L with modulation frequency of 2.6820745 GHz and amplitude 16.4 dBm

(b) The 50GHz pulse train of MLF8L with modulation frequency of 2.6820745 GHz and ac FM modulation index 0.45

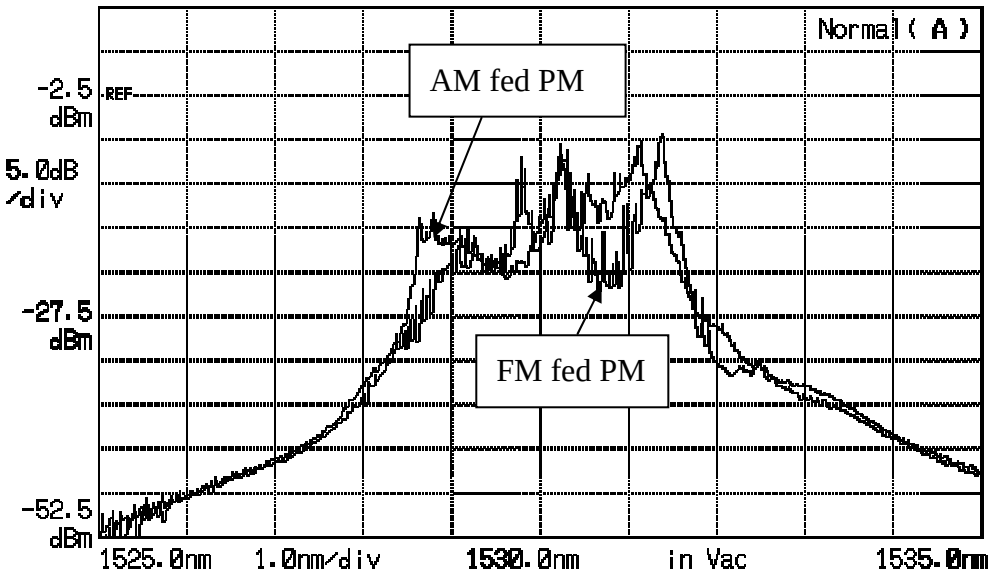

Fig. 3-27 The 50 GHz lasing spectrum with modulation frequency of 2.6820745 GHz

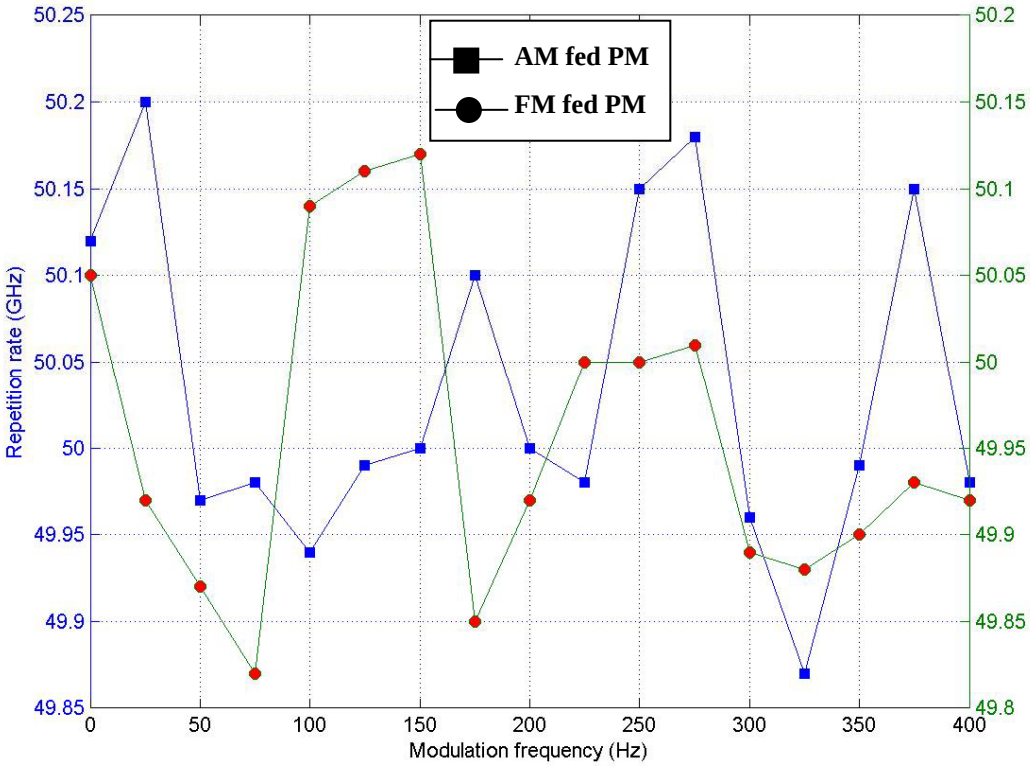

Fig. 3-28 Change of repetition rate by detuning modulation frequency. (Offset=2.6820731 GHz)

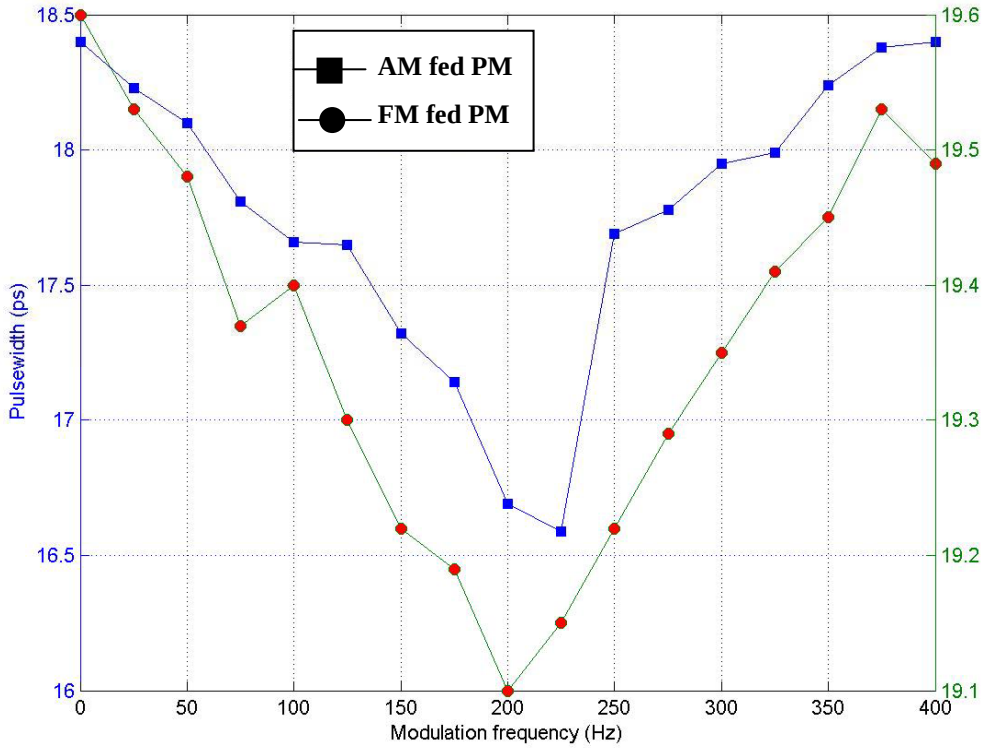

Fig. 3-29 Change of pulsewidth by detuning modulation frequency (Offset=2.6820731 GHz)

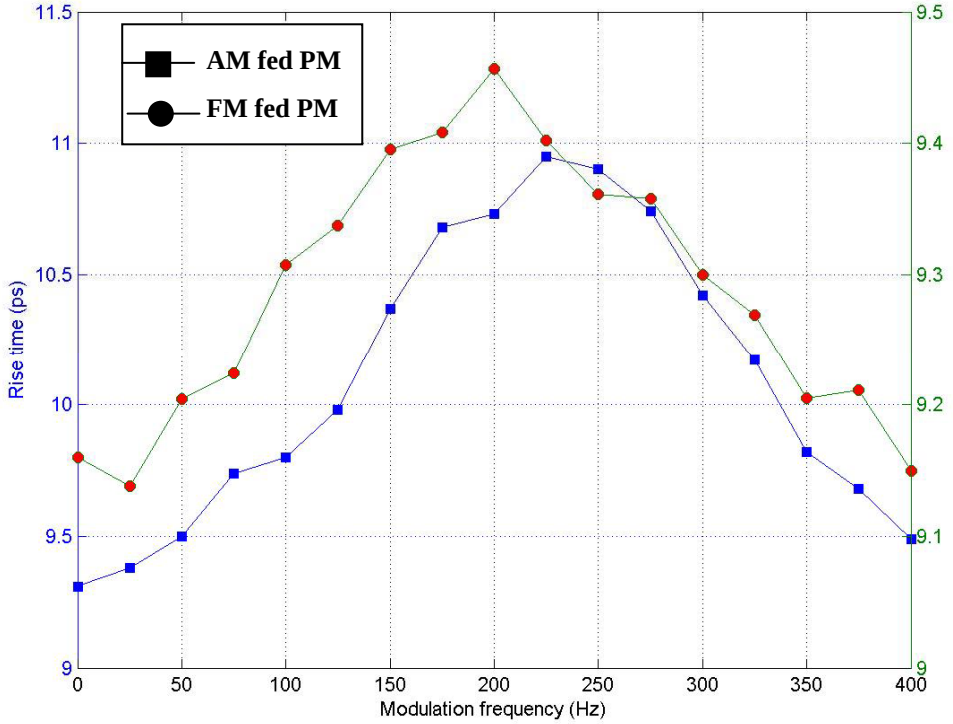

Fig. 3-30 Variation of rise time by detuning modulation frequency (Offset=2.6820731 GHz)

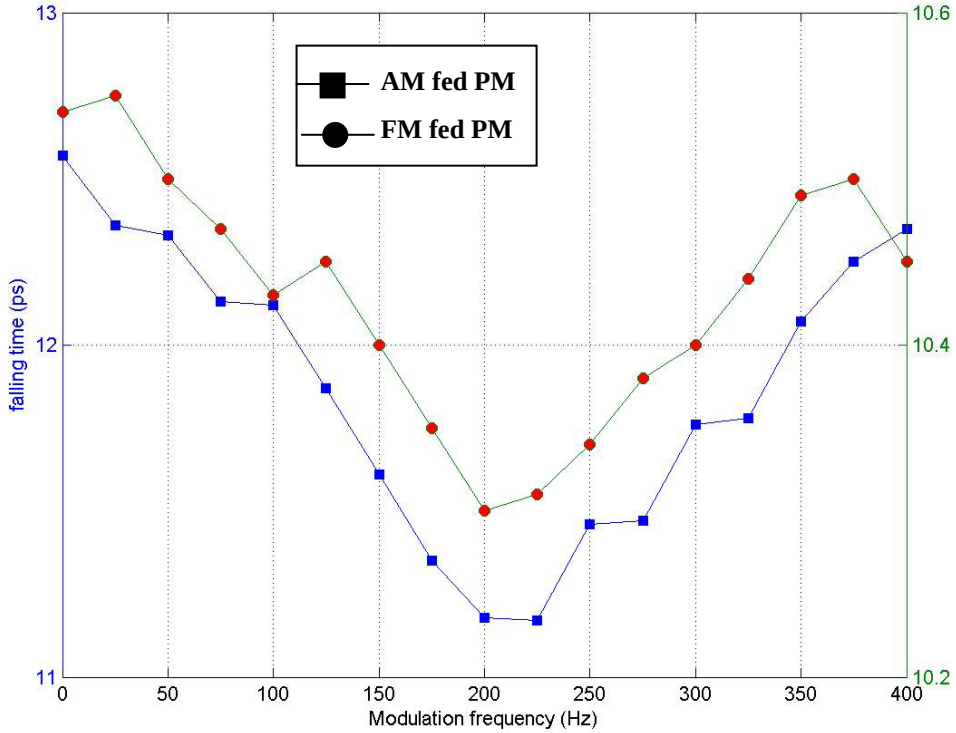

Fig. 3-31 Variation of falling time by detuning modulation frequency (Offset=2.6820731 GHz)

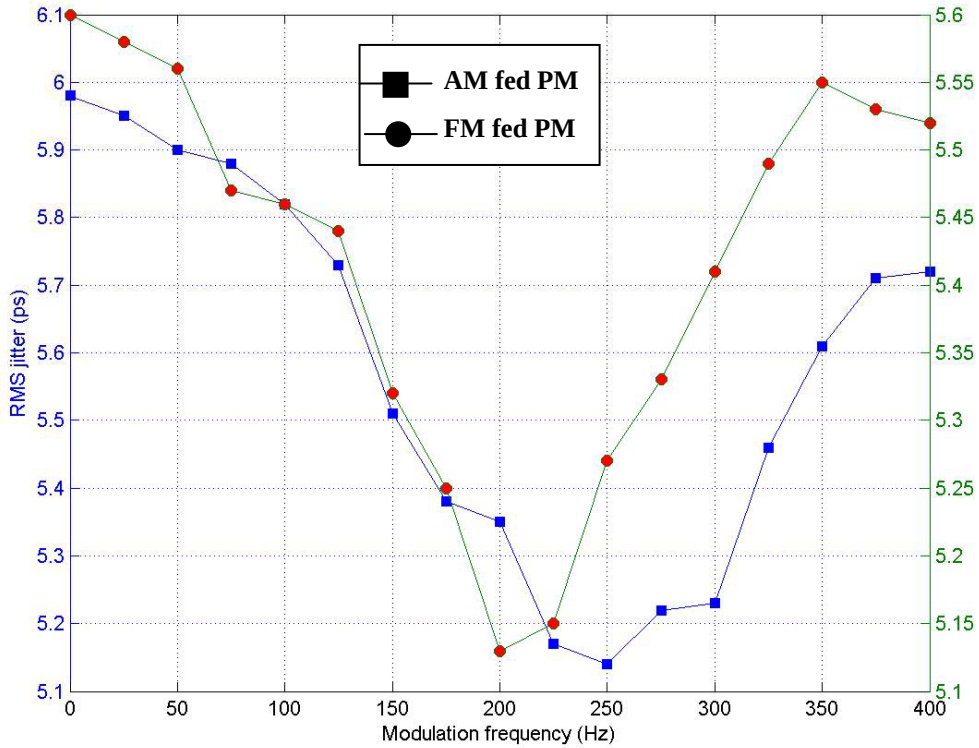

Fig. 3-32 Variation of RMS jitter by detuning modulation frequency (Offset=2.6820731 GHz)

Table 3-1

	Elements	Time Domain ABCD Matrix
1	Phase modulator	$\begin{pmatrix} 1 & 0 \\ i4\pi^2 mf^2 & 1 \end{pmatrix}$
2	SMF with dispersion	$\begin{pmatrix} 1 & -i\beta_S'' L_S \\ 0 & 1 \end{pmatrix}$
3	SMF with nonlinearity	$\begin{pmatrix} 1 & 0 \\ i\frac{2\gamma_S \bar{P} L_S}{\sqrt{\pi} f \tau^3} & 1 \end{pmatrix}$
4	EDF with dispersion	$\begin{pmatrix} 1 & -i\beta_E'' L_E \\ 0 & 1 \end{pmatrix}$
5	EDF with nolinearity	$\begin{pmatrix} 1 & 0 \\ i\frac{2\gamma_E \bar{P} L_E}{\sqrt{\pi} f \tau^3} & 1 \end{pmatrix}$

Table 3-2

Parameter	Symbol	Value
Second-order dispersion of SMF	β_S''	-1.86x10^{-26} sec^2/m
Second-order dispersion of EDF	β_E''	-1.46x10^{-26} sec^2/m
Length of SMF	L_S	64.19 m
Length of EDF	L_E	9 m
Nonlinear coefficient of SMF	γ_S	0.002 (m・W)$^{-1}$
Nonlinear coefficient of EDF	γ_E	0.02 (m・W)$^{-1}$
Average power	$\overline{P}$	3.326 mW
Modulation depth	m	0.1
Modulation frequency	f	1 GHz~2.7 GHz
Split number of EDF	M	100
Split number of SMF	N	100